3D nonlinear PET-CT image registration algorithm with constrained Free-Form Deformations

Oscar Camara, Olivier Colliot, Gaspar Delso, Isabelle Bloch

3D nonlinear PET-CT image registration algorithm with constrained Free-Form Deformations

O. Camara O. Colliot G. Delso I. Bloch

Département TSI, CNRS URA 820
Ecole Nationale Supérieure des Télécommunications
France
{Oscar.Camara, Olivier.Colliot, Gaspar.Delso, Isabelle.Bloch}@enst.fr

Abstract

This paper presents a 3D nonlinear PET-CT image registration method guided by a B-Spline Free-Form Deformations (FFD) model, dedicated to thoracic and abdominal regions. It is divided into two stages: one FFD-based registration of structures that can be identified in both images; and a whole-image intensity registration step constrained by the FFD computed during the first step. Different similarity criteria have been adopted for both stages: Root Mean Square (RMS) to register recognized structures and Normalized Mutual Information (NMI) for optimizing the whole-image intensity stage. Structure segmentation is performed according to a hierarchical procedure, where the extraction of a given structure is driven by information derived from a simpler one. This information is composed of spatial constraints and expressed by the means of regions of interest, in which a 3D simplex mesh deformable model based method is applied. The results have been very positively evaluated by three medical experts.

1. Introduction

In oncology, the joint use of anatomical and functional images is increasing, which can be explained both by the development of acquisition devices and methods, and by the complementarity between such modalities. On the functional side, the development of Positron Emission Tomography (PET) acquisitions with fluorine 18 fluorodeoxyglucose (18-FDG) tracer gives access to a rich information for diagnosis and therapeutic follow-up of both primary and metastatic cancers. But the anatomical information is reduced, making difficult to localize the tumors with a high precision with respect to the organs. This anatomical information is provided by Computed Tomography (CT) or Magnetic Resonance Imaging (MRI) and allows the physician to get an accurate localization of the lesions, as well as size and shape measures. Unfortunately it does not provide sufficient knowledge about the lesion malignancy. Therefore, combining information from these two modalities would have a significant impact on improving medical decisions for diagnosis, therapy and treatment planning [1]. Such a combination calls for a registration step in order to achieve a good correspondence between the images and the structures they contain.

The aim of this paper is to propose a contribution to the registration of CT and PET images for thoracic and abdominal applications. For such problems, rigid registration is not sufficient since it does not account for the strong deformations existing between both images, and it is necessary to develop nonrigid registration methods. These deformations, induced by the specificities of the acquisitions, are mainly due to the different acquisition protocols involved and the elastic nature of the imaged regions.

We first present a brief review of nonlinear registration algorithms. We then discuss the segmentation procedure and describe the registration method for segmented structures and for grey-level intensities. Finally, some results and a discussion of the technique are presented.

2 Registration framework

The goal of image registration is to determine the transformation that maps the information contained in one image into its anatomical correspondence in the other. Image registration methods can be divided according to several criteria: area of interest, nature of the transformation, similarity measure and optimization method. An exhaustive review of registration methods can be found in [2].

Several nonlinear transformations can be found in the image processing literature. B-Spline Free Form Deformations (FFD) is a parametric model which provides a flexible nonlinear transformation due to the fact that no assumptions on the images or structures to register are made. This model have been successfully used in different medical imaging

applications, such as pre-and post contrast MR mammogram registration [3], brain registration [4] or cardiac segmentation [5]. In general, they perform a linear transformation before the nonlinear phase to get closer enough to the final solution. Anyway, most of these applications work with monomodality data, where relationship between corresponding intensities in both images to register is simpler than in multimodality applications. This fact is aggravated when functional images are considered due to the large amount of noise and artifacts. Nevertheless, Mattes et al. [6] have used the FFD model to register chest transmission PET-CT images, applying a hierarchical and multiresolution scheme to avoid local minima and to alleviate the need for accurate initialization. One problem of this method is that it considers a functional relation between transmission and emission PET image acquisitions. Besides, authors point out that results are not satisfactory in the regions with larger deformations, such as at the diaphragm and the abdomen.

One way to avoid this problem is to constrain these deformations to avoid the convergence towards local minima and to reduce the computational cost of the algorithm. These constraints led us to propose a methodology divided into an initialization phase registering segmented structures from both images, and a second registration based on the whole-image intensities, refining the previous phase. Transformations in both steps are modeled by means of Free Form Deformations (FFD), governed by a grid of several control points for each dimension. The segmentation step is achieved by a 3D simplex mesh deformable model over regions of interest in a hierarchical identification procedure.

3 Structure segmentation

3.1 Overview of the procedure

The initial registration step requires the segmentation of some thoracic and abdominal structures in both images. This first registration will then be refined using grey-level information. Possible segmentation errors will not be propagated to the final result, as the fine registration step will be able to correct them.

Different levels of difficulty in the segmentation of structures suggest the use of a hierarchical procedure: the extraction of a given structure will be driven by information derived from a simpler one. This information can be composed of spatial constraints inferred from the previously segmented structures and be expressed by the means of Regions Of Interest (ROI) in which the search for new structures will take place. The structures to be segmented for further registration are lungs, kidneys and liver (in this order). Although they will not be used in the registration process, the skin and skeleton are also extracted as first steps of the hierarchical procedure in the case of CT images.

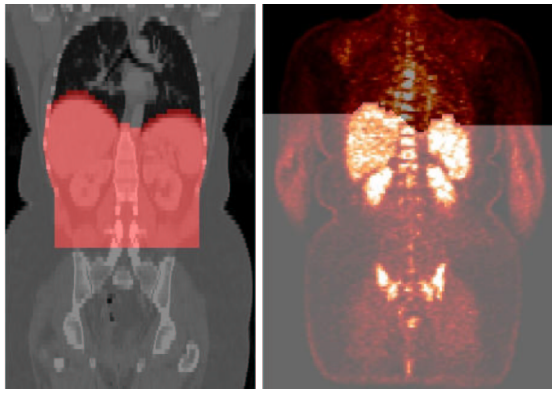

Figure 1: ROI used for the segmentation of the kidneys (brighter area). Left: CT image. Right: PET image.

Lungs, kidneys and liver are treated in two different stages: a first stage is composed of automatic thresholding and mathematical morphology operations in the ROI defined by previously segmented objects. The second stage consists in refining the result using a 3D deformable model. Skin and skeleton are segmented using only the first stage.

3.2 First stage: rough segmentation

To constrain the segmentation, a ROI is defined using spatial relationships with respect to other structures. These relationships include directions (for example the liver is below the lungs) and exclusion constraints (previously obtained structures are subtracted from the ROI so that no pair of objects overlap). The ROI for each structure are defined as follows (see Figure 1 for examples of ROI):

- skin and skeleton: they constitute the first steps of the procedure in CT and therefore no ROI is used. To locate the pelvis, we compute the area of the bounding box of the skeleton on each axial slice. The first significant decrease of this size (starting from the bottom) gives an indication of the top of the pelvis;

- lungs: in CT, the ROI is derived from the skin. In PET, we segment the lungs on the transmission image and dilate them to produce a ROI in the emission image;

- kidneys: in CT images, the region is bounded using the chest dimensions we have learned from the segmentation of the skeleton. An upper bound in the z axis is derived from the lungs: the ROI is defined below a line linking the lower-left limit of the right lung and the lower-right limit of the left lung (a line is drawn on each coronal slice). A lower bound can be computed using the top of the pelvis extracted from the skele-

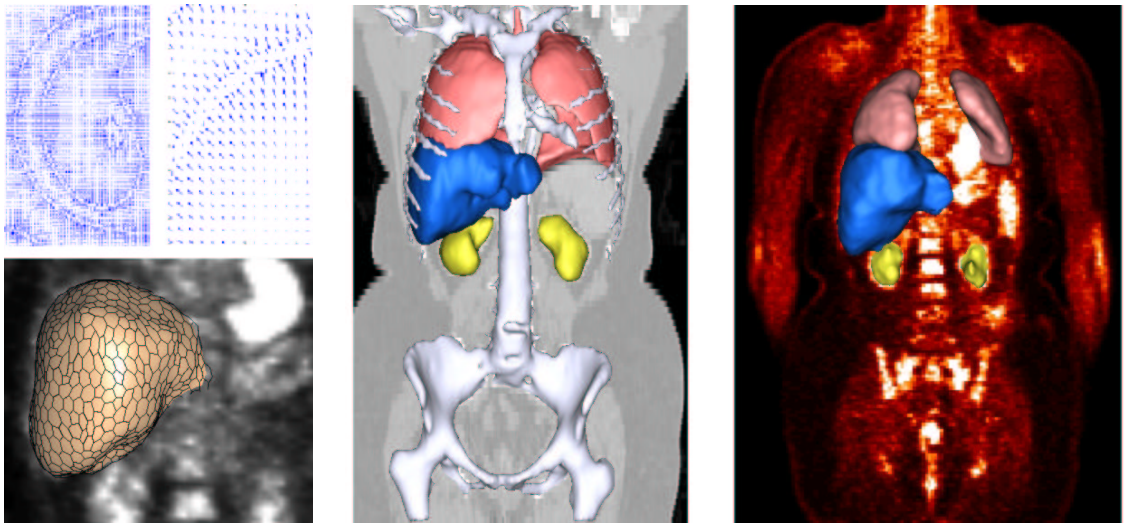

Figure 2: Top-left: Axial slice of GVF computed on a CT image (left) and detail (right). Bottom-left: Example of a simplex mesh. Middle: 3D rendering of segmented structures in CT image superimposed on a slice. Right: 3D rendering of segmented structures in PET image superimposed on a slice.

ton. In PET images, as the skeleton is not available, we only use the upper bound derived from the lungs;

- liver: the ROI is the same as above except that it excludes the kidneys. The ROI has been particularly useful to separate it from the heart and the kidneys.

Within this defined region, we then perform the following pipeline: k-means automatic thresholding, binary erosion, selection of connected components, binary dilation and 3D hole filling. In the case of the lungs and the liver, we select the biggest connected components while for the kidneys the two most symmetrical components with respect to the body symmetry plane are extracted using an algorithm proposed in [7].

3.3 Second stage: refinement using a 3D deformable model

The first stage cannot be considered as a final segmentation. The main problem is the lack of regularization term. This has proven to be a problem in the case of subtle structures which could be detected in one modality but not in the other, thus introducing a difference that the registration process would wrongly interpret as a deformation and would try to compensate. A 3D deformable model has been implemented to overcome this problem. Deformable models are curves or surfaces defined within an image that evolve under constraints computed from the image data and regularity constraints.

We chose to implement a discrete model based on simplex meshes (introduced by Delingette [8]). As a good initialization is very useful to achieve a fast convergence of the model, an initial surface is derived from the first segmentation stage. The segmentation obtained at the first stage can be eroded to ensure that the initialization is inside the object. Then, it is transformed to a triangulation using an isosurface algorithm [9]. It is decimated and converted to a simplex mesh using the dual operation.

The evolution of the deformable surface $\mathbf{X}$ is described by the following dynamic force equation:

$$\frac{\partial \mathbf{X}}{\partial t} = \mathbf{F}_{int}(\mathbf{X}) + \mathbf{F}_{ext}(\mathbf{X}) \tag{1}$$

where $\mathbf{F}_{int}$ is the internal force that specifies the regularity of the surface and $\mathbf{F}_{ext}$ is the external force that drives the surface towards image edges. The chosen internal force is:

$$\mathbf{F}_{int} = \alpha \nabla^2 \mathbf{X} - \beta \nabla^2 (\nabla^2 \mathbf{X}) \tag{2}$$

where α and β respectively control the surface tension (prevent it from stretching) and rigidity (prevent it from bending) and ∇^2 is the Laplacian operator.

In our case, the external force is not only derived from image edges but also constrains the deformable model to stay in the ROI. It can be written as a linear combination:

$$\mathbf{F}_{ext} = \lambda \mathbf{v} + \mu \mathbf{F}_{ROI} \tag{3}$$

where $\mathbf{v}$ is a Gradient Vector Flow (GVF) (introduced by Xu et al. [10]), $\mathbf{F}_{ROI}$ is a force attached to the ROI and λ and μ are weighting parameters. A GVF field is computed by diffusion of the gradient vector of a given edge map.

The edge map is derived from the gradient after performing an anisotropic diffusion. Anisotropic diffusion [11] is

an efficient way to remove noise in homogeneous regions while preserving and even enhancing edges, which proves to be very helpful for noisy structures such as the liver in PET images.

The second term of the external force is used to prevent the deformable model from going outside the ROI. $\mathbf{F}_{ROI}$ is a distance potential force and it can be written as follows:

$$\mathbf{F}_{ROI}(x) = -\frac{\nabla d(x)}{\|\nabla d(x)\|} \quad (4)$$

where d is a distance map to the ROI (the force is switched-off inside the ROI). It should be noted that we also use the ROI as a mask on the GVF and thus the GVF is equal to zero outside the ROI. Finally, we also use the ROI as a mask on the obtained segmentation to ensure that no objects are overlapping. Segmentation results are shown in Figure 2.

4 Nonlinear registration procedure

4.1 Overview

The nonlinear registration procedure is separated into two stages: the first step consists of the registration between segmented structures in both images; and the second step, initialized with the precedently computed transformation, performs a refined registration between the whole intensity images.

4.2 Deformation model

A nonlinear transformation based on B-Spline Free Form Deformations (FFD), introduced by Sederberg et al. [12], has been chosen to establish the correspondence between images. The choice of this method over other more constrained parametric models is due to the great variability of the structures in our application. So, we preferred the flexibility that FFDs get from the fact that no assumptions on the structures are made. On the other hand, the speed requirements of the system make FFDs preferable to other more realistic and time consuming deformation frameworks, such as elastic or fluid models.

In this technique, deformations of the object volume are achieved by tuning an underlying mesh of control points. The number of control points would define the locality of the deformations allowed by the FFD model. On the other hand, convergence times will notably increase with a more densely populated grid. Thus, a trade-off concerning these two aspects must be taken, our choice being a mesh of 10 control points for dimension.

FFD model has been used for both stages of the registration procedure. This implementation allows us to easily integrate the two phases into the same framework, structures registration being considered as just an extra step of the multiresolution chain used in most voxel-based techniques. Thus, fine registration procedure will start with the grid found in the structure registration phase, which provides an initial transformation very close to the final solution, at least in the neighborhood of the segmented structures.

The optimization procedure is based on an iterative gradient descent technique over the entire grid of control points. At each iteration, we compute a local gradient estimation for each control point by finite differences. Furthermore, a local spring force regularization term has been added to prevent the nodes from intersecting, which could lead to unwanted alterations of the structure topology.

4.3 Structure registration

The aim of this step is to provide an initialization to the grey-level registration as close as possible to the desired final result. This transformation will constrain the search of the global solution that will undergo the next stage. Therefore, this registration phase can be seen as a multiresolution step, filtering out of all the data but the main structures, then forwarding the result as an initial estimate to a higher level where finer detail will be considered.

Before performing nonlinear registration between anatomical features, we compute an initial approximation of the transformation between both images. This approximation is composed of a rigid motion, an independent scaling along the three axes and the elimination of the parts of the volumes that have no interest for our application.

The FFD framework implies tuning the control points of the grid to minimize a given similarity criterion. The choice of this criterion is straightforward in our case, as we are working with segmented images with a linear intensity relation. Thus, the Root Mean Square (RMS) difference of corresponding pixel grey levels, summed across the whole volume, will be used to determine the optimal deformation parameters.

An overlap measure consisting of the quotient between intersection and union among structures (being equal to 1 if total superimposition is achieved) has been used to evaluate CT and nonlinear registered PET recognized features. We have obtained a value of 0.658 for the linear phase and a value of 0.903 for the nonlinear phase, clearly improving structure registration results, as can be seen in Fig. 3.

4.4 Fine registration

Transformation produced by the initialization step is not necessarily valid for those regions away from the segmented structures, so the computation of their displacement has to be done by this fine registration stage. Another objective of this stage is the correction of the errors that may have been

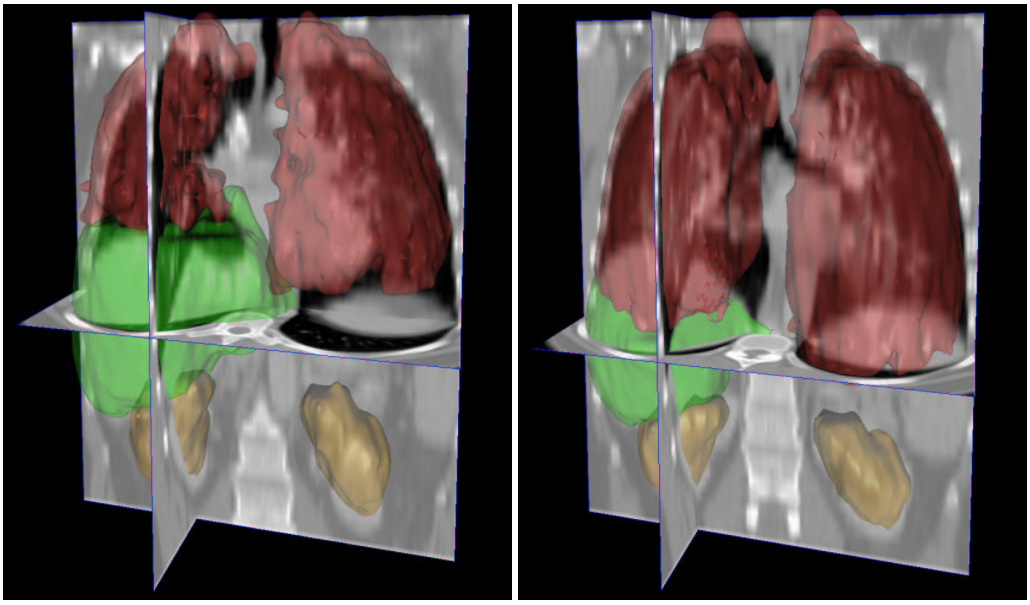

Figure 3: Example of structure registration. Left: 3D rendering of PET segmented structures after rigid registration with slices from CT original image. Right: 3D rendering of PET segmented structures after nonlinear structure registration with slices from CT original image, illustrating the extent of the deformation.

introduced by the structure segmentation procedure, taking advantage of the image grey level information.

As the deformation framework has not changed, the algorithm is essentially the same as the one used in the structure registration stage. Nevertheless, the fact of working with the whole image intensity levels forces us to change the similarity criterion to maximize. The choice of a similarity measure is strongly related to the imaging modalities to be registered. A particularly complex situation arises when the intensity distributions of two different modalities do not follow a functional relation, such as in our case, implicating PET and CT images. Mutual Information (MI), a criterion proposed by Viola [13], has been demonstrated to be a powerful tool for multimodal image registration with a nonlinear intensity relation. MI expresses how much information from an image I is contained in another image J. Therefore, Mutual Information will be maximal if the images are geometrically aligned. NMI is a variant of MI, introduced by Studholme [14] to prevent the actual amount of image overlap from affecting the measure. Its computation requires an estimation of the marginal and joint probability distributions from both images. We use a frequency-based approximation, $p_{ij} = n_{ij}/n$, where p_{ij} is the estimated probability of having an intensity *i* in one image and *j* in the other, n_{ij} being the number of voxels with these intensities and *n* the total number of voxels.

5 Results and conclusions

We tested our method on a set of 15 CT and PET scans of the thoracic and abdominal regions. Some slices of the superimposition between CT and registered PET image can be seen in Figure 4 (All slices can be found at: http://www.tsi.enst.fr/ ocamara/Evaluation3.html). We have devised an evaluation protocol which has allowed a group of three clinicians (Dr.Foehrenbach, Dr. Rigo and Dr. Marchandise) to assess the registration results using an online procedure. The measure generated provides an error less than 1cm over the most relevant structures (lungs, liver, kidneys, heart), which conforms to the objective of the application (errors smaller than PET resolution images).

We have verified that the registration is better achieved around segmented structures which have been already registered in the initialization stage, independently of its belonging to thoracic or abdominal zones. One exception is the errors found in the stomach because of its important movements between two acquisitions and the fact that no constraints have been imposed on it, thus NMI registration has not converged towards the correct registration. The fact of constraining the FFD deformation by means of an initialization stage has speed up the convergence of the fine registration step, the computational cost being reduced over 80%.

As a conclusion, the results presented in this paper indicate that our method can provide an useful tool for data analysis in thoracic and abdominal oncology applications.

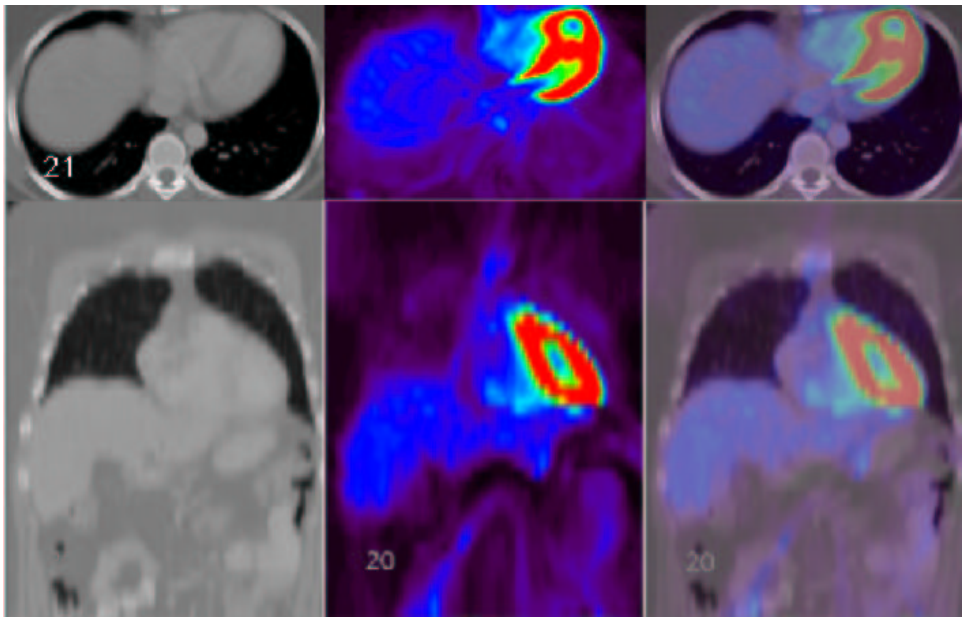

Figure 4: An axial and a coronal slice of registration results. Left: CT original image. Center: Registered PET image. Right: Superimposition of both images. All slices can be found at: http://www.tsi.enst.fr/ ocamara/Evaluation3.html

The nonrigidity in the imaged regions is effectively modeled by means of a Free Form Deformation (FFD), and satisfactory registration results can be obtained by minimizing a Normalized Mutual Information criterion, given a good enough initialization. A progressive segmentation method has been proposed to provide such an initialization, integrating it as a first step of the multiresolution procedure.

Further work will focus on allowing the initialization phase to assign a weight to the nodes of the FFD according to the mechanical properties of the underlying tissue.

Acknowledgments

The authors would like to thank Dr. Hervé Foehrenbach, Dr. Pierre Rigo, Dr. Xavier Marchandise, Yves Martelli, the research team of S.H.F.J. in Orsay and the members of Segami Corporation for their contribution to this project. This work was partially supported by the French Ministry for Research (grant number 01B0267).

References

[1] H. N. Wagner, "Fused Image Tomography: An Integrating Force," *Nuclear Medicine*, vol. 40, no. 8, pp. 13N–32N, 1999.

[2] J. B. A. Maintz and M. A. Viergever, "A Survey of Medical Image Registration," *Medical Image Analysis*, vol. 2, no. 1, pp. 1–36, 1998.

[3] D. Rueckert, I. Somoda, C. Hayes, D. Hill, M. Leach, and D. Hawkes, "Nonrigid Registration Using Free-Form Deformations: Applications to Breast MR Images," *IEEE Transactions on Medical Imaging*, vol. 18, no. 8, pp. 712–721, 1999.

[4] T. Hartkens, D. Hill, A. Castellano-Smith, D. Hawkes, C. M. Jr., A. Martin, W. Hall, H. Liu, and C. Truwit, "Using points and surfaces to improve voxel-based non-rigid registration," in *MICCAI*, 2002, pp. 565–572.

[5] J. Lotjonen, "Segmentation of MR images using deformable models: Application to cardiac images," *International Journal of Bioelectromagnetism*, vol. 3, no. 2, pp. 37–45, 2001.

[6] D. Mattes, D. R. Haynor, H. Vesselle, T. K. Lewellen, and W. Eubank, "Pet-ct image registration in the chest using free-form deformations," *IEEE Transactions on Medical Imaging*, vol. 22, no. 1, pp. 120–128, 2003.

[7] O. Colliot, I. Bloch, and A. Tuzikov, "Characterization of approximate plane symmetries for 3D fuzzy objects," in *IPMU*, vol. 3, Annecy, France, July 2002, pp. 1749–1756.

[8] H. Delingette, "General object reconstruction based on simplex meshes," *International Journal of Computer Vision*, vol. 32, no. 2, pp. 111–146, 1999.

[9] W. Lorensen and H. Cline, "Marching cube, a high resolution 3D surface reconstruction algorithm," in *SIGGRAPH 87*, vol. 21, no. 3, pp. 163–169.

[10] C. Xu and J.-P. Prince, "Gradient vector flow: A new external force for snakes," in *CVPR97*, Puerto Rico, June 1997, pp. 66–71.

[11] G. Gerig, O. Kubler, R. Kikinis, and F. Jolesz, "Nonlinear anisotropic filtering of MRI data," *IEEE Transactions on Medical Imaging*, vol. 11, no. 2, pp. 221–232, June 1992.

[12] T. Sederberg and S. Parry, "Free form deformation of solid geometric models," in *SIGGRAPH'86*, vol. 20, Dallas, USA, August 1986, pp. 151–160.

[13] P. Viola and W. Wells, "Alignment by maximization of mutual information," *International Journal of Computer Vision*, vol. 24, no. 2, pp. 137–154, 1997.

[14] C. Studholme, D. Hill, and D. Hawkes, "An overlap invariant entropy measure of 3D medical image alignment," *Pattern Recognition*, vol. 32, pp. 71–86, 1999.